JOURNAL OF MATERIALS SCIENCE 14 (1979) 2975–2980

Micromechanics of crack nucleation during indentations

J. T. HAGAN
Physics and Chemistry of Solids, Cavendish Laboratory, Madingley Road, Cambridge, CB3 OHE, UK

An analysis for the nucleation of microcracks from the inhomogeneous flow lines in soda-lime glass under Vickers indentations is considered. The minimum loads for crack nucleation are shown to depend on the hardness, H, and the critical stress intensity factor, K_{IC}. Unlike the Lawn and Evans analysis, the present model does not require the presence of any fortuitous flaws of critical dimensions in the material, since the flaws are nucleated by the deformation in the deformed zone.

1. Introduction

The formation of median cracks during indentations with a Vickers indenter consists of the nucleation of the initiating flaw in the bulk and its subsequent propagation. The propagation of the fully developed median cracks has been discussed extensively by several workers [1–7]. The problem of the nucleation of the flaw is, however, more complex because of the elastic–plastic indentation stress fields involved. This is further complicated by the fact that when dealing with crystalline solids, material properties like grain size, hardness, H, and the critical stress intensity factor, K_{IC}, would be expected to influence the nucleation processes.

The initiation of the median crack has been considered recently by Lawn and Evans [2]. Their model implies the existence of sub-surface "fortuitous" flaws of the right critical dimensions in the vicinity of the elastic–plastic boundary where the indentation tensile stresses are highest. By making assumptions about the magnitude (from Hill's treatment [8]) and variation of the tensile stresses and the location of the initiating pre-existing cracks, Lawn and Evans have obtained critical conditions for the initiation of the sub-surface flaws. They have shown that the minimum load to propagate the critical flaws is

$$P_C = 2.2 \times 10^4 \left(\frac{K_{IC}}{H}\right)^3 K_{IC}. \quad (1)$$

The size of the corresponding "fortuitous" critical flaw is given by

$$C_{min} = 44.2 \left(\frac{K_{IC}}{H}\right)^2. \quad (2)$$

In the above model, failure of the expanding tensile stress front to meet the right critical flaw means that the applied load has to be increased so that the expanding tensile front can sample flaws which lie deeper in the bulk. The magnitude of the tensile stress level stays constant and it is only its position that varies in order to sample the randomly distributed flaws in the bulk. Their treatment, however, ignores the response of the materials to the constraints on the deformation imposed by the indenter, and disregards any anisotropy or inhomogeneity in the deformation of crystalline materials. Moreover, the minimum crack lengths predicted by this model of 123 μm for NaCl and 440 μm for KCl are large enough to be detected if they really existed in the "virgin" material. It is proposed in this paper that these large flaw sizes are not necessarily inherent in the materials, and that the interaction of dislocations in crystalline materials [9–13] or inhomogeneous deformation in some glassy materials [1] can play an important role in the nucleation and growth of the sub-surface cracks to the large sizes predicted by the Lawn and Evans model.

0022–2461/79/122975–06$02.60/0

2. Observations on crack nucleation in solids

The importance of inhomogeneity in the sub-surface deformation and the interaction of shear flow lines to the nucleation of both median and lateral cracks around Vickers indentations in soda-lime glass has been pointed out by Hagan and Swain [1]. More recent studies of the sub-surface deformed zones under Vickers indentations in single crystals of LiF and KCl have again highlighted the importance of the deformation process to the nucleation of various cracks around the indentations. Fig. 1 shows the surface and sub-surface deformation around Vickers indentations in LiF. The method of sectioning the indentations is described elsewhere [1, 14]. The haloes arrowed H on the surface of the specimen in Fig. 1a are reflections from sub-surface cracks around the 10 N load indentation on the sectioning crack, SS. Fig. 1c to f show the sub-surface deformations in LiF at indenter loads of 5, 10, 25 and 30 N, respectively. The specimens have been etched in a dilute solution of $FeCl_3$ in distilled water to reveal the dislocations. The cracks, SC, along (1 0 1) 45° appear at indenter loads of 10 N and they are obviously formed by the interaction of dislocations on intersecting (1 1 0) 90° and (1 0 1) 45° planes (Fig. 1d). The median crack, MC in Fig. 1f, formed at loads of 30 N, is again the result of the interaction of dislocation on two intersecting (1 0 1) 45° planes. Fig. 2 shows the sub-surface deformation under Vickers indentations in KCl. The specimen has not been etched and the sub-surface deformation is uniform and radial from the indenter faces. The deformed sub-surface region is similar to that observed in cold-rolled steel under

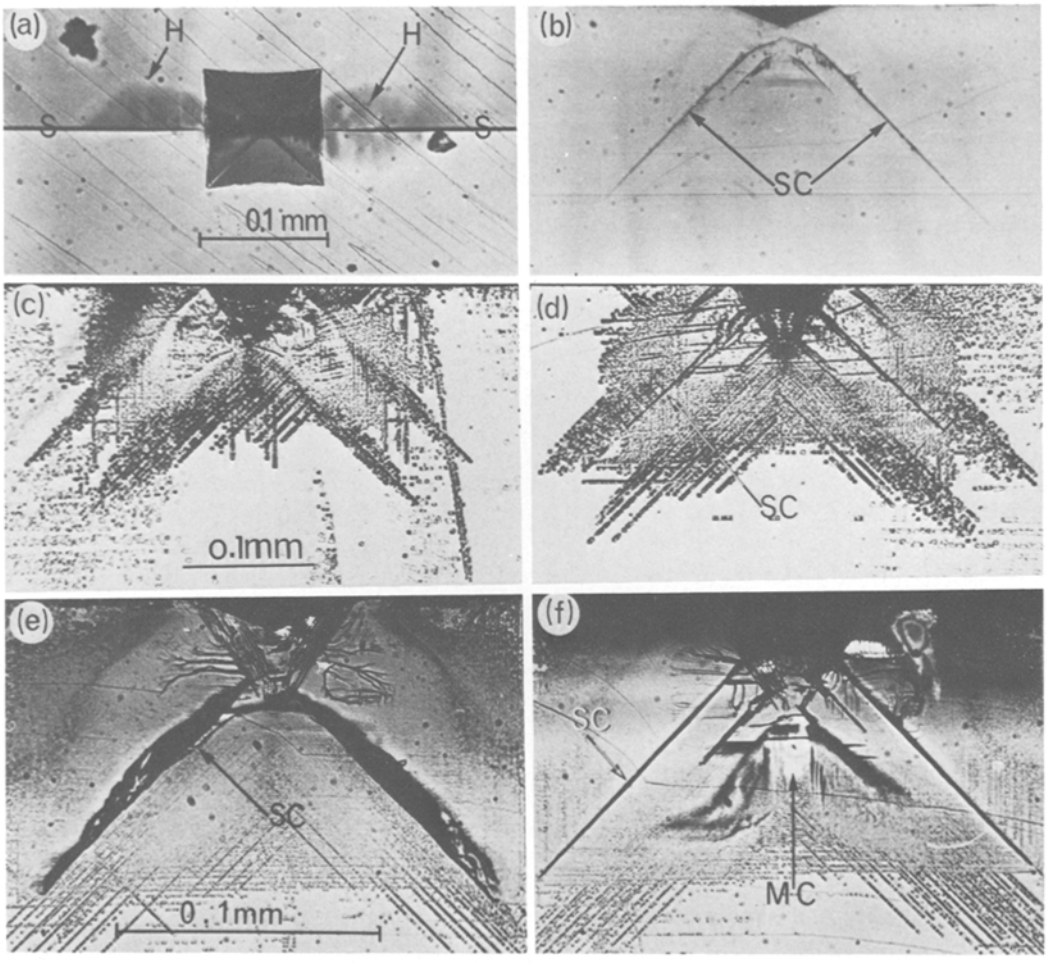

Figure 1 Surface (a) and sub-surface (b) damage under Vickers indentations in LiF. (c), (d), (e) and (f) are etched surfaces of sub-surface regions under Vickers indenter at loads of 5, 10, 25 and 30 N, respectively. Shear cracks are marked SC in (b) and (d) and the median crack is arrowed MC in (f).

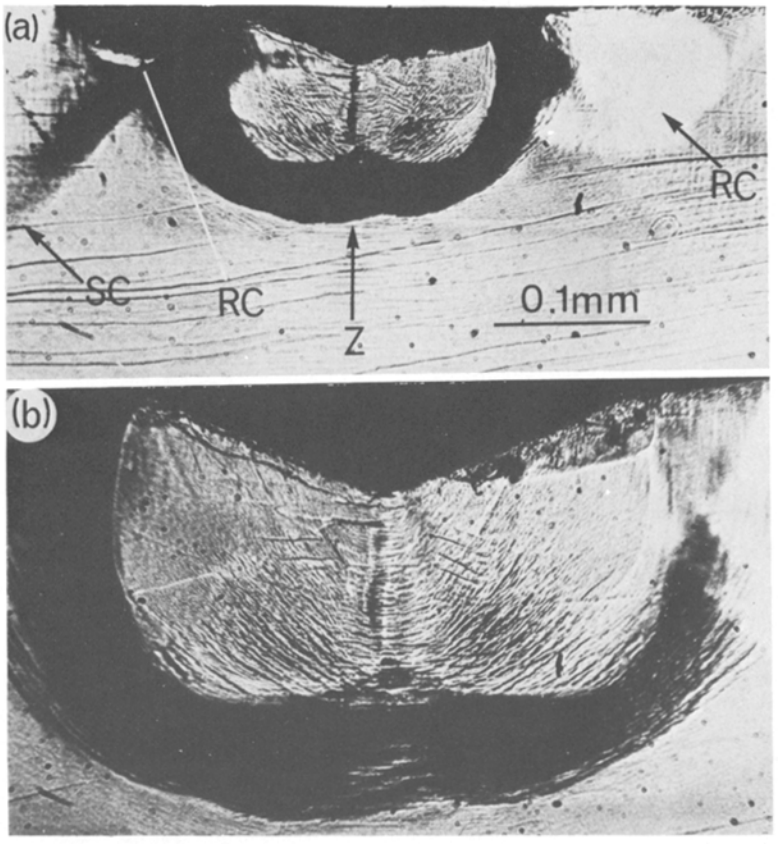

Figure 2 Unetched sub-surface damage under 50 N load Vickers indentations in KCl; (b) higher magnification of deformed zone. Palmqvist radial cracks and shear cracks are marked RC and SC respectively in (a).

wide-angle wedge indentations by Mulhearn [15]. The radial cracks, RC, appear to start at the boundary of the intense deformation band and there are traces of what appear like 45° cracks marked SC in Fig. 2a; Fig. 2b is a higher magnification of the deformed zone in Fig. 2a. A more detailed account of the nucleation of the various crack systems around pyramidal indentations in a range of solids is in preparation [16].

It is thus apparent that deformation processes can play a major role in crack nucleation in crystalline solids or other materials which deform inhomogeneously. Further, nucleation is likely to be controlled on a more localized scale than is afforded by the expanding tensile stress front model of Lawn and Evans.

3. Theory

A model proposed for crack nucleation under Vickers indentation is based essentially on crack nucleation from the interaction of dislocations on two intersecting slip planes or from one slip plane blocking dislocations on another slip plane [9–13]. Since the nucleation is governed by shear deformation, tensile stresses do not appear to play an important part in the nucleation of these cracks.

Consider a number of dislocations piling up at a point O due to slip on the plane OS and shear stress, σ_S (see Fig. 3). The normal stress at point P (associated with such a pile up) and acting normally on a plane inclined at θ to the slip plane is

$$\sigma = \sigma_S \left[\frac{L}{r}\right]^{1/2} f(\theta), \qquad (3)$$

where L is the slip length, r is the distance of P from O and $f(\theta)$ gives the angular dependence [10]. For isotropic solids this stress has a maximum value for $\theta = 70.5°$. A singularity occurs in the stress field and near the end of the pile up the stresses may be high enough to lead to the rupture of cohesive bonds in the region of the high stress concentration. One may also compute the energy associated with forming a hypothetical crack, c, along OP and determine whether the formation

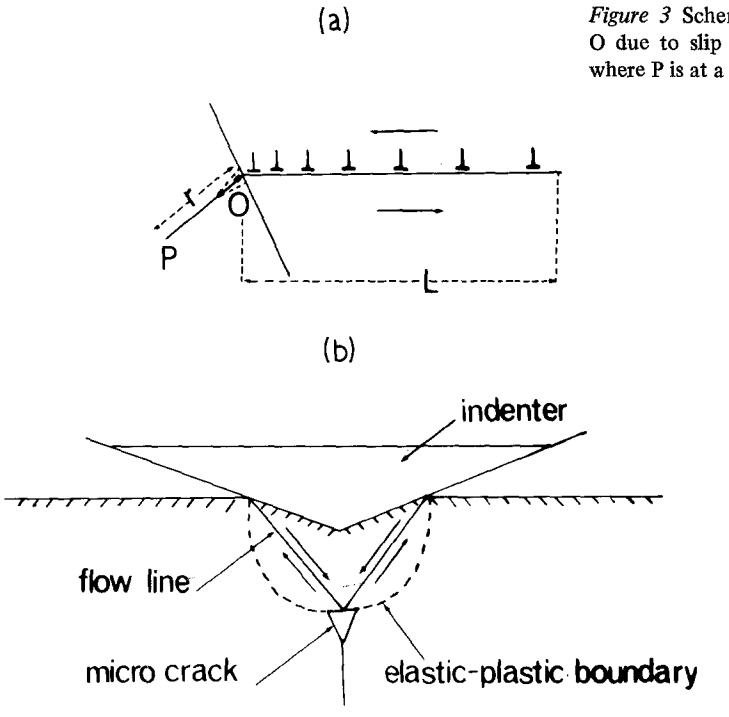

Figure 3 Schematic diagram of dislocations piling up at O due to slip along OS and producing a crack along OP where P is at a distance of r from O.

of such a crack would lead to an overall decrease in the energy associated with the pile up [10].

It has been shown that the dislocations in the pile up will collapse and coalesce to form a crack (with an overall decrease in energy) if the effective shear stress as given by Stroh is

$$\sigma_S^2 = \frac{3\pi}{8}\left[\frac{\gamma\mu}{(1-\nu)L}\right], \qquad (4)$$

where γ is the fracture surface energy, μ is the shear modulus, and ν is the Poisson ratio. This equation is independent of the crack length and is, therefore, satisfied for all crack lengths much less than L. This means that when the critical conditions for crack nucleation are satisfied, the cracks continue to grow in size until the elastic energy associated with the dislocation pile up has been dissipated in creating new fracture surfaces.

To calculate the critical conditions for microcrack nucleation using Vickers indentation one assumes that:

(a) the slip length, L, for the nucleation of a crack is less than or equal to $1.4a$ where a is half the diagonal length of the indentation (experimental observation); and

(b) the operating shear stress has a maximum value equal to the shear yield stress, which for a perfectly rigid-plastic solid is $H/6$ (H is the hardness).

This assumption is justified by the fact that under spherical indentations on LiF single crystals, the resolved stress on the dislocation nearest the specimen surface is $0.1H$ [17]. Stroh has also shown that in polycrystalline metals the dislocation-induced cracks can form at strains within the elastic limit and the operating shear stresses are likely to be lower than $H/6$.

In the treatment that follows, it will be assumed the $\sigma_s = 0.1H$. This means that Equation 4 becomes

$$H^2/100 = 3\pi E\mathscr{G}/32(1-\nu^2)L \qquad (5)$$

where $\mathscr{G}$ ($= 2\gamma$) is the strain energy release rate and E is the Young's modulus. The equation $\mu = E/2(1+\nu)$ relating μ and E is, of course, strictly true for isotropic solids only, but it is assumed to be reasonably accurate if mean values of μ, E and ν are taken. Equation 5, therefore, represents conditions of crack initiation if the formation of such a crack would lead to an overall decrease in the energy of the system.

Since the critical stress intensity factor, K_{IC}, is related to the strain energy release rate, $\mathscr{G}$, by

$$K_{IC}^2 = \frac{E\mathscr{G}}{1-\nu^2}$$

for plane strain conditions, Equation 5 may be expressed as

$$L = \frac{3\pi \times 100}{32}\left[\frac{K_{IC}}{H}\right]^2 = 29.5\left[\frac{K_{IC}}{H}\right]^2. \quad (6)$$

As pointed out earlier, Stroh's analysis [10] holds for all crack lengths much less than L, the slip length. To obtain the maximum crack length allowed by this analysis, we set the slip length L in Equation 6 equal to the crack length. This is equivalent to setting the maximum crack length equal to the grain size in polycrystalline materials [10]. Therefore,

$$c = 29.5\left[\frac{K_{IC}}{H}\right]^2. \quad (7)$$

Also, since $L \simeq 1.4a$ and the Vickers hardness, H is given by

$$a = \left[\frac{P}{2H}\right]^{1/2}. \quad (8)$$

Equation 8 may be substituted into Equation 6 to obtain the critical load for crack nucleation of

$$P_c = 885\left[\frac{K_{IC}}{H}\right]^3 K_{IC}. \quad (9)$$

Equations 7 and 9 are essentially the same as those given by Lawn and Evans model except for the constants in the expressions. The differences in the constants arise from the choice of the maximum operating stresses. The critical loads P_c and the largest crack sizes that could be formed by such dislocation processes for various materials are listed and compared with those given by the Lawn and Evans analysis (see Table I).

4. Discussion

The above analysis assumes that it is the continued slip on the inhomogenous flow or slip line that is responsible for the nucleation and growth of the crack to the critical dimensions. In general, however, the applied load will have a tensile component normal to and across the crack path and this would contribute to the propagation of the crack. For a given critical load the crack lengths given in Table I are likely to be lower estimates. Two main points can be made concerning the present analysis and the results of Table I. Firstly, a mechanism for producing flaws during the deformation process is provided. This removes a major problem of the Lawn and Evans model, which, for materials such as NaCl and KCl, required very large flaws of detectable dimensions to be present. Secondly, though it must be appreciated that the data in Table I from both models are only approximate, the new model predicts rather lower values for P_c than for the Lawn and Evans.

It seems likely that a material property like grain size should influence the nucleation parameters. However, it appears that in these indentation experiments the effects of grain size is implicit in the overall response of the material to the indenter constraints through the hardness H and the position of the elastic–plastic boundary where the maximum distortions can occur. The

TABLE I

Materials	Hardness H (GPa)	K_{IC} (MPa m$^{1/2}$)	Critical load (N)		Critical flaw (μm)	
			Lawn and Evans	Present analysis	Lawn and Evans	Present analysis
Wc (Cb	18.6	13.0	98	39.4	22	14.4
NaCl (sc)	0.24	0.4	41	1.6	123	82
KCl (sc)	0.095	0.3	208	8.4	440	295
Si_3N_4 (hp)	16.0	5.0	3.3	0.14	4.3	2.9
Al_2O_3	12.0	4.0	3.3	0.13	5	3.3
ZnS (vd)	1.9	1.0	3.2	0.12	12.2	8.2
SiC (hp)	19.0	4.0	0.8	0.03	2	1.3
MgF_2 (hp)	5.8	0.9	0.07	0.03	1.1	0.7
MgO (hp)	9.2	1.2	0.06	0.25	0.8	0.58
SiO_2	6.2	1.2	0.02	0.008	1.7	1.1
Si (sc)	10.0	0.6	0.003	0.001	0.2	0.1

Cb, Co-bonded; sc, single crystal; hp, hot-pressed; vd, vapour-deposited.

high compressive hydrostatic pressure directly below the indenter effectively limits or suppresses any micro-structural effects to regions at the elastic–plastic boundary.

The application of this model, which is strictly only true for crystalline materials, to glassy silicates calls for comment. In glasses, like soda-lime glass, which display inhomogeneous flow properties under pyramidal indentations [17], the analysis may be used without too much error. The use of the model for predicting critical conditions in fused silica glass, which does not exhibit any inhomogeneous flow characteristics under pyramidal indentations [18], is uncertain. No detailed analysis has been made for this situation, but stresses at the elastic–plastic boundary caused by the wedging action of the deformed zone may cause flaws to develop.

The analysis assumes that the shear stresses involved in crack nucleation are approximately $0.1H$. For highly elastic solids like glasses, the shear yield stress in fact usually lies between 0.3 and $0.4H$. It is, however, possible that the yield stress or yield behaviour of silicate glasses in compression is different from that in tension because of the possible compaction of the silica network in compression experiments. The true yield stress may, therefore, be lower than with other glasses and nearer to the assumed value of $0.1H$.

It is worth pointing out that a recent analysis by Veldkamp *et al.* [19] has shown that the minimum load for the nucleation of cracks around scratches is

$$F = L\frac{K_{IC}^4}{H_S^3}$$

where H_S is the scratching hardness and L is a constant for a given geometry and the orientation of the scratching point and for a particular crack. This equation is essentially the same as given by Lawn and Evans and in this paper (Equation 9); and it underlies the basic processes of microplasticity and fracture in both static and scratching experiments.

Acknowledgements

The author is grateful to Drs J. E. Field, M. M. Chaudhri and M. V. Swain for useful discussions and comments on the paper. This work was supported by the Ministry of Defence (Procurement Executive) and the Science Research Council.

References

1. J. T. HAGAN and M. V. SWAIN, *J. Phys. D. Appl. Phys.* **11** (1978) 2091.
2. B. R. LAWN and A. G. EVANS, *J. Mater Sci.* **12**, (1977) 2195.
3. B. R. LAWN and E. R. FULLER, *ibid.* **10** (1975) 2016.
4. B. R. LAWN and M. V. SWAIN, *ibid.* **10** (1975) 113.
5. H. E. EXNER, *Trans. Met. Soc. AIME* **245** (1969) 677.
6. A. G. EVANS, *J. Amer. Ceram. Soc.* **59** (1976) 371.
7. A. G. EVANS and T. R. WILSHAW, *Acta Met.* **24** (1976) 939.
8. R. HILL, "The Mathematical Theory of Plasticity", (Clarendon Press, Oxford, 1950).
9. C. ZENER, *Trans. ASM* **40** (1948) 2.
10. A. N. STROH, *Adv. Phys.* **6** (1957) 192.
11. A. H. COTTRELL, *Trans. Met. Soc. AIME* **212** (1958) 192.
12. J. A. WILLIAM, *Acta Met.* **15** (1967) 1559.
13. A. S. KEH, J. C. M. LI and Y. F. CHOU, *ibid* **7** (1959) 694.
14. K. W. PETER, *J. Non. Cryst. Solids* **5** (1970) 103.
15. T. O. MULHEARN, *J. Mech. Phys. Solids* **7** (1959) 85.
16. J. T. HAGAN, (1979) to be published.
17. M. V. SWAIN, *Wear* **48** (1978) 173.
18. J. T. HAGAN, *J. Mater. Sci.* **14** (1979) 462.
19. J. D. B. VELDKAMP, N. HATTU and V. A. C. SNIJDERS, "Fracture Mechanisms of Ceramics", Vol. 3, edited by R. C. Bradt, D. P. D. Hasselman and F. F. Lange (Plenum Press, New York, London, 1978).

Received 10 May and accepted 24 May 1979.